TRACK VIBRATIONS DURING ACCELERATING AND DECELERATING PHASES OF HIGH-SPEED RAILS

K. K. ANG [1*], T. M. THI[2†], and L. V. HAI[3]

[1, 2]*Department of Civil and Environmental Engineering, National University of Singapore, Singapore*

[3]*Department of Civil Engineering, Ho Chi Minh City University of Technology, Vietnam National University - Ho Chi Minh, Vietnam*

ABSTRACT

In this paper, a computational study using the moving element method (MEM) was carried out to investigate the dynamic response of a high-speed rail (HSR). A new formulation for calculating the general mass, damping and stiffness matrices of the moving element is proposed. Resonance in the vibration response of the rail track is found to occur during both the accelerating and decelerating phases of the HSR. As to be expected, track vibration peaks when the HSR travels at a speed in the vicinity of the resonance velocity during the transition accelerating or decelerating phases rather than at the constant velocity phase. A parametric study is carried out to understand the effects of various factors on the response of the train-track system such as the train acceleration/deceleration magnitudes, the severity of railhead roughness and the magnitude of wheel load.

Keywords: moving element method, wheel-rail interaction, track irregularity

1. INTRODUCTION

Railway transportation is one of the key modes of travel today. The advancement in train technology leading to faster and faster trains is without doubt a positive development, which makes HSR travel more attractive as a viable alternative to other modes of transportation for long distance travel.

In dealing with moving load problems, such as that encountered in HSR, the finite element method (FEM) encounters difficulty when the moving load approaches the boundary of the finite domain and travels beyond the boundary. These difficulties can be overcome by employing a large enough domain size but at the expense of significant increase in computational time. To overcome the complication encountered by FEM, Krenk et al. (1999) proposed the use of FEM in convected coordinates to obtain the response of an elastic half-space subject to a moving load. The key advantage enjoyed by this approach is its ability to overcome the problem due to the moving load

* Corresponding author: Email: kk_ang@nus.edu.sg

† Presenter: Email: tranminhthi@nus.edu.sg

travelling over a finite domain. Andersen et al. (2001) employed the same approach to solve the problem of a beam on a Kelvin foundation subject to a harmonic moving load. Koh et al. (2003) adopted the idea of convected coordinates for solving train-track problems, and named the numerical algorithm as the moving element method (MEM). The method was subsequently applied to the analysis of in-plane dynamic response of annular disk (Koh et al. 2006) and moving loads on a viscoelastic half space (Koh et al. 2007). Recently, Ang et al. (2012) applied the MEM to investigate the "jumping wheel" phenomenon in high-speed train motion at constant velocity over a transition region where there is a sudden change of foundation stiffness.

Various researchers have investigated the problem of loads travelling at non-uniform velocities. Suzuki (1977) employed the energy method to derive the governing equation of a finite beam subject to traveling loads involving acceleration. By using analytical solutions, Yadav (1991) has investigated the vibration response of a train-track-foundation system resulting from a vehicle travelling at variable velocities. Anders Karlstrom (2006) also used an analytical approach to investigate ground vibrations due to accelerating and decelerating trains.

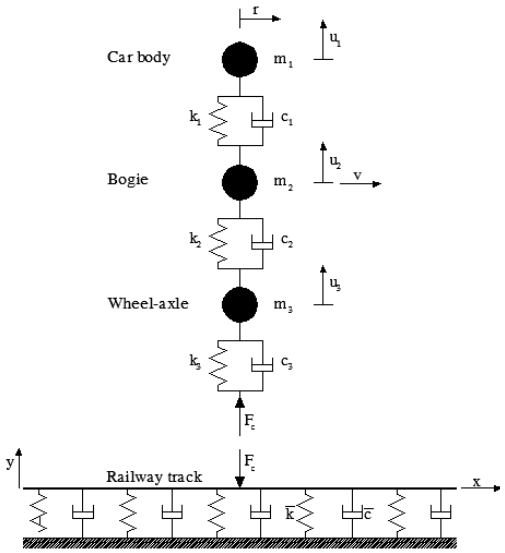

Figure 1: The HSR model

Safety concerns during the accelerating and decelerating phases of a high-speed train journey have not been adequately addressed in the literature. One major concern is the possible occurrence of resonance of the system when the frequency of the external force, in this case the rail corrugation, coincides with the natural frequency of a significant vibration mode of the system. When this happens, the response of the system is dynamically amplified and becomes significant large. This paper is concerned with a computational study of the dynamic response of HSR systems involving accelerating/decelerating trains using the MEM. A new formulation for calculating the general structural matrices of the moving element is proposed. A parametric study is performed to understand the effects of various factors on the response of the train-track system, such as the magnitudes of train acceleration/deceleration, the severity of railhead roughness and the magnitude of wheel load.

2. FORMULATION AND METHODOLOGY

The HSR system, as shown in Figure 1, comprises of a train modeled as a moving sprung-mass traversing over a rail beam in the positive x-direction. The origin of the fixed x-axis is arbitrarily located along the beam. However, for convenience, its origin is taken such that the train is at $x = 0$ when $t = 0$. The velocity and acceleration of the train at any instant are v and a, respectively. The railhead is assumed to have some imperfections resulting in the so-called "track irregularity". In the

moving sprung-mass model, the topmost mass m_1 represents the car body where the passengers are. The car body is supported by a bogie of mass m_2 through a secondary suspension system modeled by the spring k_1 and dashpot c_1. The bogie is in turn supported by a wheel-axle system of mass m_3 through a primary suspension system modeled by the spring k_2 and dashpot c_2. The contact between the wheel and rail beam is modeled by the spring k_3 and dashpot c_3. The contact force between the wheel and rail beam is denoted by F_c. The rail beam rests on a viscoelastic foundation comprising of vertical springs $\bar{k}$ and dashpots $\bar{c}$. The vertical displacement of the rail beam is denoted by y, while the vertical displacements of the car body, bogie and wheel-axle are denoted by u_1, u_2 and u_3, respectively.

The governing equation of motion of the rail beam, which is modeled as an Euler-Bernoulli beam resting on a viscoelastic foundation subject to a moving load, is given by

$$EI\frac{\partial^4 y}{\partial x^4}+\bar{m}\frac{\partial^2 y}{\partial t^2}+\bar{c}\frac{\partial y}{\partial t}+\bar{k}y=F_c\delta(x-s) \tag{1}$$

where E, I and $\bar{m}$ are the Young's modulus, second moment of inertia and mass per unit length of the rail beam, respectively; s the distance traveled by the train at any instant time t; and δ the Dirac-delta function.

The moving element method adopts the idea in which the origin of the spatial coordinates system is attached to the applied point of the moving load. Figure 1 shows a travelling *r*-axis moving at the same speed as the moving load. The relationship between the moving coordinate r and the fixed coordinate x is given by

$$r=x-s \tag{2}$$

In view of equation (3), the governing equation in equation (1) may be rewritten as

$$EI\frac{\partial^4 y}{\partial r^4}+\bar{m}\left(v^2\frac{\partial^2 y}{\partial r^2}-2v\frac{\partial^2 y}{\partial r\partial t}-a\frac{\partial y}{\partial r}+\frac{\partial^2 y}{\partial t^2}\right)+\bar{c}\left(\frac{\partial y}{\partial t}-v\frac{\partial y}{\partial r}\right)+\bar{k}y=F_c\delta(r) \tag{3}$$

By adopting Galerkin's approach and procedure of writing the weak form in term of the displacement field, the formulation for general mass $\mathbf{M}_e$, damping $\mathbf{C}_e$ and stiffness $\mathbf{K}_e$ matrices of the moving element can be determined as follows

$$\begin{aligned}
\mathbf{M}_e &= \bar{m}\int_0^L \mathbf{N}^{\mathrm{T}}\mathbf{N}\,\mathrm{d}r \\
\mathbf{C}_e &= -2\bar{m}v\int_0^L \mathbf{N}^{\mathrm{T}}\mathbf{N}_{,r}\,\mathrm{d}r+\bar{c}\int_0^L \mathbf{N}^{\mathrm{T}}\mathbf{N}\,\mathrm{d}r \\
\mathbf{K}_e &= EI\int_0^L \mathbf{N}_{,rr}^{\mathrm{T}}\mathbf{N}_{,rr}\,\mathrm{d}r+\bar{m}v^2\int_0^L \mathbf{N}^{\mathrm{T}}\mathbf{N}_{,rr}\,\mathrm{d}r-\left(\bar{m}a+\bar{c}v\right)\int_0^L \mathbf{N}^{\mathrm{T}}\mathbf{N}_{,r}\,\mathrm{d}r+\bar{k}\int_0^L \mathbf{N}^{\mathrm{T}}\mathbf{N}\,\mathrm{d}r
\end{aligned} \tag{4}$$

where the subscript r denotes partial derivative with respect to r. For beam elements, it is common to use the shape function $\mathbf{N}$ based on Hermitian cubic polynomials.

Considering the special case in which the train traverses at a constant velocity V, i.e. $a = 0, v = V$, equation (4) reduces to

$$\begin{aligned}
\mathbf{M}_e &= \bar{m}\int_0^L \mathbf{N}^{\mathrm{T}}\mathbf{N}\,\mathrm{d}r \\
\mathbf{C}_e &= -2\bar{m}V\int_0^L \mathbf{N}^{\mathrm{T}}\mathbf{N}_{,r}\,\mathrm{d}r + \bar{c}\int_0^L \mathbf{N}^{\mathrm{T}}\mathbf{N}\,\mathrm{d}r \\
\mathbf{K}_e &= EI\int_0^L \mathbf{N}_{,rr}^{\mathrm{T}}\mathbf{N}_{,rr}\,\mathrm{d}r + \bar{m}V^2\int_0^L \mathbf{N}^{\mathrm{T}}\mathbf{N}_{,rr}\,\mathrm{d}r - \bar{c}V\int_0^L \mathbf{N}^{\mathrm{T}}\mathbf{N}_{,r}\,\mathrm{d}r + \bar{k}\int_0^L \mathbf{N}^{\mathrm{T}}\mathbf{N}\,\mathrm{d}r
\end{aligned} \tag{5}$$

which are noted to be identical to the matrices derived by Koh et al. (2003).

In general, the wheel contact force F_c may be written as

$$F_c = c_3\Delta\dot{y} + k_3\Delta y \tag{6}$$

where the overdot operator denotes differentiation with respect to time and Δy, the indentation at the contact surface, can be expressed as

$$\Delta y = y_r + y_t - u_3 \tag{7}$$

in which y_r and u_3 denote the displacements of the rail and wheel, respectively, and y_t the magnitude of the track irregularity at the contact point. Note that track irregularity is a major source of the dynamic excitation. According to the recommendation by Nielsen and Abrahamsson (1992), the track irregularity profile can be written in terms of a sinusoidal function as follows

$$y_t = -a_t \sin\frac{2\pi x}{\lambda_t} \tag{8}$$

where a_t and λ_t denote the amplitude and wavelength of the track irregularity, respectively.

As the dynamic response of the train-track system depends significantly on the accuracy in modeling the contact between the wheel and track, Hertz contact theory (Esveld 2001) is employed to account for the nonlinear contact force F_c between the wheel and rail as follows

$$F_c = \begin{cases} K_H\Delta y^{\frac{3}{2}} & for \quad \Delta y \geq 0 \\ 0 & for \quad \Delta y < 0 \end{cases} \tag{9}$$

$$\text{where } K_H = \frac{2}{3}\sqrt{\frac{E^2\sqrt{R_{wheel}R_{railprof}}}{(1-\upsilon^2)^2}} \tag{10}$$

in which K_H denotes the Hertzian spring constant; R_{wheel} and $R_{railprof}$ the radii of the wheel and railhead, respectively, and υ the Poisson's ratio of the material.

The governing equations for the vehicle model are

$$\begin{aligned} m_1\ddot{u}_1 + k_1\left(u_1 - u_2\right) + c_1\left(\dot{u}_1 - \dot{u}_2\right) &= -m_1 g \\ m_2\ddot{u}_2 + k_2\left(u_2 - u_3\right) + c_2\left(\dot{u}_2 - \dot{u}_3\right) - k_1\left(u_1 - u_2\right) - c_1\left(\dot{u}_1 - \dot{u}_2\right) &= -m_2 g \\ m_3\ddot{u}_3 - k_2\left(u_2 - u_3\right) - c_2\left(\dot{u}_2 - \dot{u}_3\right) &= -m_3 g - F_c \end{aligned} \tag{11}$$

where g denotes gravitational acceleration. Upon combining equation (11) with the governing equations for the rail beam given in equation (3), the equation of motion for the train-track system may be written as

$$\mathbf{M}\ddot{\mathbf{z}} + \mathbf{C}\dot{\mathbf{z}} + \mathbf{K}\mathbf{z} = \mathbf{P} \tag{12}$$

where $\ddot{\mathbf{z}}$, $\dot{\mathbf{z}}$, $\mathbf{z}$ denote the global acceleration, velocity and displacement vectors of the train-track system, respectively; $\mathbf{M}$, $\mathbf{C}$ and $\mathbf{K}$ the global mass, damping and stiffness matrices, respectively; and $\mathbf{P}$ the global load vector. The above dynamic equation can be solved by any direct integration methods such as Newmark-β method (Bathe 1996).

3. NUMERICAL RESULTS

To verify the accuracy of the proposed MEM approach in obtaining the dynamic response of a HSR considering variable train speed, the present solutions are compared against solutions obtained by Koh et al. (2003) using the so-called 'cut-and-paste' FEM. The latter involves updating the force and displacement vectors in accordance with the position of the vehicle while keeping the structure mass, damping and stiffness matrices constant.

For the purpose of comparison only, the same train speed profile adopted by Koh et al. (2003) is employed. This speed profile is shown in Figure 2 where it can be seen that there are 3 phases of travel. The speed profile parameters for this case are presented in Table 2 under Case 1. The initial phase considers the train to be moving at a constant acceleration of travel and reaching a maximum speed of 20 m/s after 2 s. During the second phase of travel, the train moves at the maximum constant speed for another 2 s. In the final phase, the train decelerates at a constant magnitude to come to a complete halt after another 2 s of travel. Results obtained using the proposed method are found to be in excellent agreement with those obtained by the 'cut-and-paste' FEM.

In the following sections, the effects of amplitudes of train acceleration/deceleration, track irregularity and wheel load on dynamic response of the train-track system during the accelerating or decelerating phases using the proposed MEM approach are presented. The parameters for various train speed profiles considered are presented in Table 2 under cases 2 to 4. The proposed MEM model adopted in the study comprises of a truncated railway track of 50 m length uniformly

discretized into 250 moving finite elements. Values of parameters related to the properties of track and foundation are summarized in Table 1 (Koh et al. 2003). The equations of motion are solved using Newmark's constant acceleration method employing a time step of 0.0005s. This small time step size is necessary in view of the inherent high natural frequency of the train-track system. In analyses involving the Hertz nonlinear contact model, Newton-Raphson's method (Bathe 1996) is employed to solve the resulting nonlinear equations of motion. The radii of the wheel R_{wheel}, railhead $R_{railprof}$ and the Poisson's ratio of the wheel/rail material υ used in determining the nonlinear Hertz spring constant are taken to be 460 mm, 300 mm and 0.3, respectively.

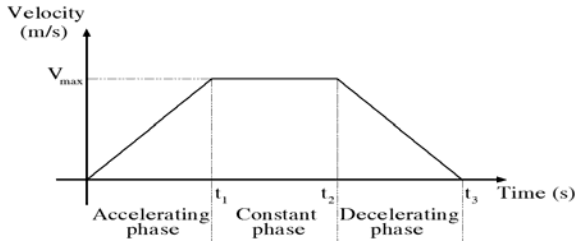

Figure 2: Profile of train speed

Table 1: Parameters for track-foundation model

Parameter	Value
Flexural stiffness	6.12×10^6 N m^2
Track section	UIC 60 (60 E1)
Stiffness of foundation	1×10^7 N/m^2
Damping ratio	0.1

Table 2: Profiles of train velocities

Case	Maximum velocity V_{max} (m/s)	Amplitude of acceleration/deceleration $\lvert a \rvert$ (m/s^2)	Time parameters		
			t_1 (s)	t_2 (s)	t_3 (s)
1	20	10	2.0	4.0	6.0
2	70	0.600	117.0	119.0	236.0
3	70	0.720	98.0	100.0	198.0
4	70	2.222	31.5	33.5	65.0

3.1. Effect of amplitudes of train acceleration/acceleration

As the stiffness matrix of the moving element and the track irregularity depend on the train acceleration or deceleration amplitudes, it is necessary to investigate the effect of the amplitudes on the dynamic amplification factor (DAF) in wheel-rail contact force. Note that three amplitudes of train acceleration/deceleration (Cases 2, 3 and 4), as shown in Table 2, and three track irregularities such as smooth (0.01 mm), moderate (0.5 mm) and severe (2 mm) are considered. Note that the wavelength of all track irregularities is chosen to be 1 m. Figure 3 shows the effect of train acceleration/deceleration amplitudes on the DAF. The results obtained show that the magnitude of acceleration/deceleration has negligible effect on the DAF for all cases considered. In view of this finding, all other results to be subsequently presented shall pertain to case 3, considered to be the typical speed profile of today's HSR travels.

3.2. Effect of track irregularity amplitude

The effect of track irregularity amplitude on the DAF is next investigated. Note that the wavelength λ_t of all track irregularities is chosen to be 1 m. In order to compare the DAF obtained at resonant

speed during accelerating/decelerating phases, it is necessary to determine the DAF when the train travels at the constant resonant speed computed as λ_t / T, where T is the period of the system. Figure 4 shows how track irregularity amplitude affects the DAF. For a near smooth track ($a_t = 0.01$ mm), the DAF is found to be approximately 1, as to be expected. When the amplitude of track irregularity increases, the DAF is noted to increase gradually and then significantly. It is interesting to note that the DAF is found to be higher during both the accelerating and decelerating phases as compared to the case in which the train travels at a constant speed equal to the resonant speed. The DAF is also noted to be slightly larger during the decelerating phase as compared to the accelerating phase.

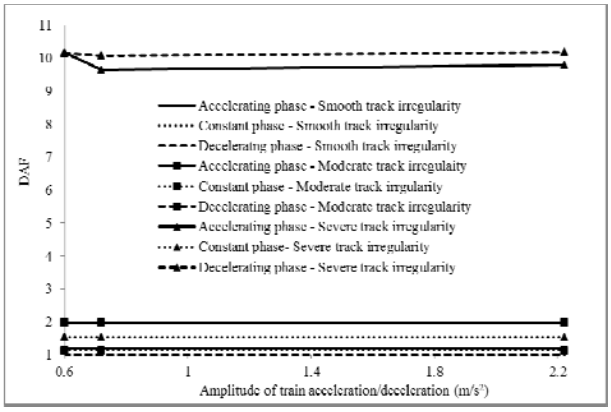

Figure 3: Effect of amplitudes of train acceleration/deceleration on the DAF.

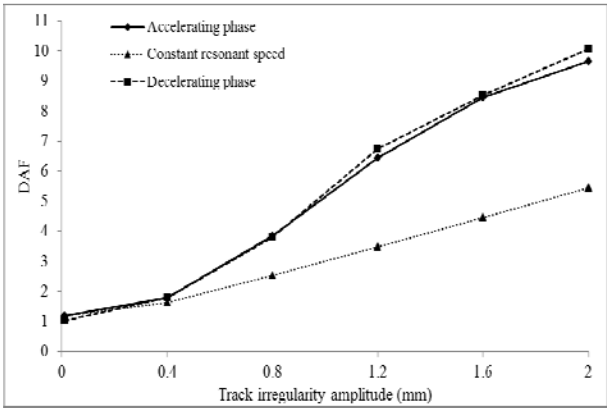

Figure 4: Effect of track irregularity amplitude on the DAF.

3.3. Effect of track irregularity wavelength

As the period of HSR system is fixed, the magnitude of track irregularity wavelength is a significant factor on controlling the occurrence of the resonant phenomenon during the accelerating and decelerating phases. Resonance occurs briefly during accelerating/decelerating phases when the train speed reaches the magnitude of the resonant speed. This occurs when the maximum train speed is higher than the resonant speed.

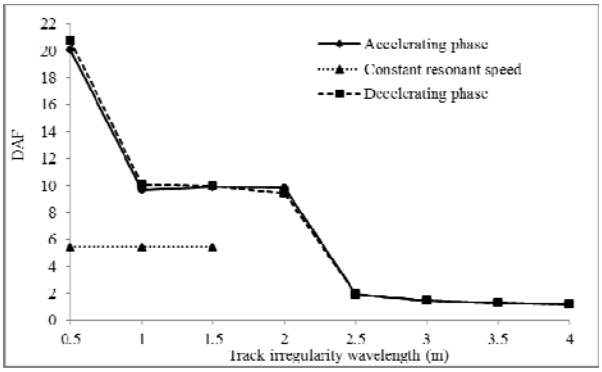

Figure 5: Effect of track irregularity wavelength on the DAF.

Figure 5 shows the effect of track irregularity wavelength on the DAF. Note that all irregularity amplitudes considered are 2 mm. It is expected that shorter irregularity wavelength would lead to larger vibrations as can be observed when the wavelength is small at 0.5 m. When the

wavelength of track irregularity increases, the DAF is found to decrease. It is interesting to note that the DAF is higher during both the accelerating and decelerating phases as compared to the case in which the train travels at a constant speed equal to the resonant speed.

3.4. Effect of wheel load

The effect of wheel load on dynamic response of the system is next investigated. Two wheel loads of 41 kN and 81 kN are considered. The smaller load corresponds to the case of a very lightly loaded vehicle (Koh et al. 2003), and the higher load corresponds to a typical passenger vehicle. Figure 6 shows the effect of wheel load on the DAF for various values of track irregularity amplitude. Note that the wavelength of all track irregularities is chosen to be 1 m. It is expected that the lighter wheel load is, the larger DAF is, especially for the larger track irregularity amplitude. Using various values of track irregularity wavelength, Figure 7 shows the effect of wheel load on the DAF. In this case, the amplitude of all track irregularities is chosen to be 2 mm. It is also expected that the DAF is larger when the wheel load is lighter, especially for the smaller track irregularity wavelength.

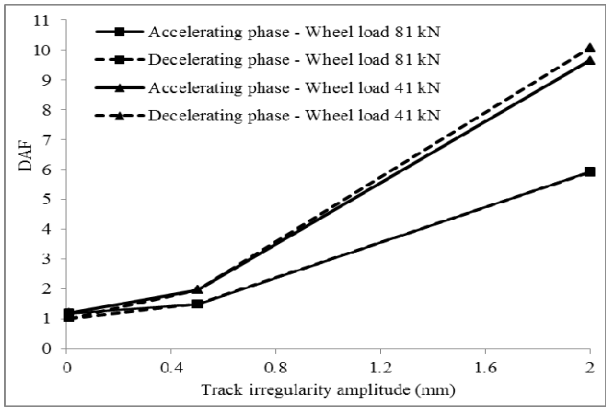

Figure 6: Effect of wheel load and track irregularity amplitude on the DAF.

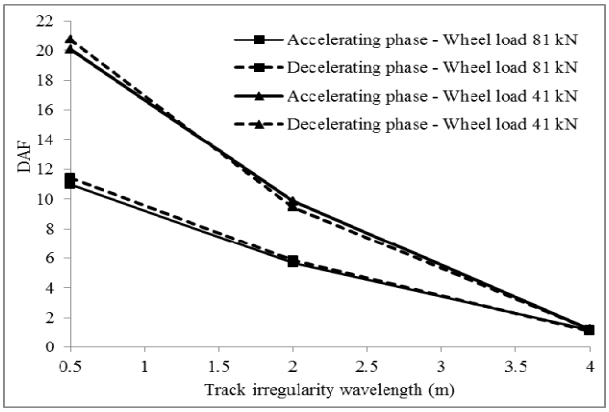

Figure 7: Effect of wheel load and track irregularity wavelength on the DAF.

4. CONCLUSIONS

In this paper, a numerical study on the dynamic response of HSR system using the moving element method was carried out. A new and general formulation for calculating the structural matrices of the moving element was proposed. The effects of magnitudes of train acceleration/deceleration, track irregularity and wheel load to response of HSR system during a train journey are investigated.

The results obtained using the proposed MEM is found to agree well with results found in the literature using the 'cut-and-paste' FEM. It is found that the magnitude of acceleration/deceleration has negligible effect on the DAF. The DAF is more increasing when the irregularity amplitude/wavelength is more increasing/decreasing. As to be expected, the DAF are larger when the HSR travels at a resonant speed during the accelerating/decelerating phases rather than the case

in which the train travels at a constant speed equal to the resonant speed. When the wheel load is lighter, the DAF is larger, especially for the severe track irregularity.

5. ACKNOWLEDGMENTS

This research is funded by Vietnam National University Ho Chi Minh City (VNU-HCM) under grant number B2013-20-07.

REFERENCES

Suzuki SI (1977). Dynamic behavior of a finite beam subjected to travelling loads with acceleration. Journal of Sound and Vibration. 55(1), pp. 65–70.

Yadav D (1991). Non-stationary dynamics of train and flexible track over inertial foundation during variable velocity. Journal of Sound and Vibration. 147(1), pp. 57–71.

Anders Karlstrom (2006). An analytical model for ground vibrations from accelerating trains. Journal of Sound and Vibration. 293, pp. 587–598.

Krenk S, Kellezi L, Nielsen SRK, and Kirkegaard PH (1999). Finite elements and transmitting boundary conditions for moving loads. Proceedings of the 4th European Conference on Structural Dynamics, Eurodyn ‘99, Praha, June 7-1, Vol. 1, pp. 447-452.

Andersen L, Nielsen SRK, and Kirkegaard PH (2001). Finite element modelling of infinite Euler beams on Kelvin foundations exposed to moving loads in convected co-ordinates. Journal of Sound and Vibration. 241(4), pp. 587-604.

Koh CG, Ong JSY, Chua DKH, and Feng J (2003). Moving Element for Train-Track Dynamics. International Journal for Numerical Methods in Engineering. 56, pp. 1549-1567.

Koh CG, Sze PP, and Deng TT (2006). Numerical and analytical methods for in-plane dynamic response of annular disk. International Journal of Solids and Structures. 43, pp. 112-131.

Koh CG, Chiew GH, and Lim CC (2007). A numerical method for moving load on continuum. Journal of Sound and Vibration. 300, pp.126-138.

Ang KK, Dai J, and Thi TM (2012). Analysis of high-speed rail accounting for jumping wheel phenomenon. The International Conference on Advances in Computational Mechanics (ACOME), August 14-16, Ho Chi Minh City, Vietnam.

Nielsen JCO and Abrahamsson TJS (1992). Coupling of physical and modal components for analysis of moving non-linear dynamic systems on general beam structures. International Journal for Numerical Methods in Engineering. 33, pp. 1843-1859.

Esveld C (2001). Modern Railway Track (2nd Edition). MRT Productions: Duisburg.

Bathe KJ (1996). Finite Element Procedures. Prentice-Hall, Englewood Cliffs, N.J.